East European Journal of Physics. 2. 476-481 (2026)
DOI:10.26565/2312-4334-2026-2-53 ISSN 2312-4334

STRUCTURAL, MORPHOLOGICAL, AND OPTICAL PROPERTIES OF ZnO THIN FILMS GROWN ON Si SUBSTRATES VIA ULTRASONIC SPRAY PYROLYSIS

Azim K. Soatov[1]*, Abdumajit R. Turayev[1], Azamat O. Arslonov[2]
[1]*Center for Development of Nanotechnologies, National University of Uzbekistan*
[2]*Department of Physics, National University of Uzbekistan, Tashkent 100174, Uzbekistan*
**Corresponding Author e-mail: soatovazim36@gmail.com*
Received March 1, 2026, revised April 10, 2026; accepted April 14, 2026

Based on scientific sources presenting modern semiconductor device fabrication technologies and growth methods, the influence of external factors on ZnO samples was evaluated through various approaches. In this work, ZnO thin films were grown on Si substrates using the ultrasonic spray pyrolysis (USP) method. The physical characteristics of the obtained samples, including the optical bandgap energy and in-situ laser Raman spectroscopy measurements, were investigated. The primary objective of this study was to synthesize ZnO thin films with precise nanometric thicknesses on silicon (Si) substrates and to investigate the influence of substrate temperature, precursor composition, and evaporation rate. Using Ellipsometry, XRD, and SEM, we characterized the film thickness, crystal lattice structure, and morphological evolution during growth.
Keywords: *Silicon; Zinc oxide; Crystal structure; Molar concentration; Bandgap*
PACS: 81.15.Rs

INTRODUCTION

Zinc oxide (ZnO) is a semiconductor characterized by a wide direct bandgap, with an energy of approximately 3.37 eV at room temperature. This value significantly exceeds the bandgap energies of conventional diamond-structured semiconductors such as Si, Ge, and GaAs. These unique properties enable the development of a new generation of nanomaterials. Consequently, ZnO is considered a promising material for optoelectronic devices, including ultraviolet (UV) photodetectors, light-emitting diodes (LEDs), transparent conducting oxides, pressure sensors, and next-generation memory elements [1]. The exciton binding energy of ZnO is approximately 60 meV, which is relatively high. This results in strong exciton emission even at room temperature, thereby enhancing the efficiency of its application in light-emitting devices [2,3].

Various methods have been developed to synthesize ZnO thin films with diverse morphological and structural properties. These include sol-gel spin-coating, hydrothermal growth, chemical vapor deposition (CVD), and spray pyrolysis [4]. Among these techniques, ultrasonic spray pyrolysis (USP) has gained particular attention for its simplicity, cost-effectiveness, and ability to control film thickness and composition over large areas [5]. This method allows for precise control over the precursor solution concentration, which significantly influences the crystal structure, defect density, and optical properties of the ZnO films [6]. It is well known that defects within the ZnO structure, specifically oxygen vacancies (V_O) and zinc interstitials (Zn_i), strongly affect its optical and electronic properties [7]. These defects create localized energy levels within the bandgap, resulting in defect-related emissions in the visible spectrum and altering the overall quality of the film. Previous studies have demonstrated that increasing the precursor concentration during deposition enhances crystalline quality, reduces defect density, and improves photoluminescence properties [8,9]. The aim of this research is to investigate how the molar concentration of the precursor affects the structural and optical properties of ZnO thin films deposited via the USP method. By analyzing the variations in crystallinity, morphology, and photoluminescence behavior across different molar concentrations, this study explores the potential to optimize ZnO thin films for advanced optoelectronic applications [10].

2. MATERIALS AND METHODS

2.1. Substrate Preparation

Zinc oxide (ZnO) thin films were deposited on Si (100) oriented silicon substrates using the ultrasonic spray pyrolysis (USP) technique. Prior to the deposition process, the silicon substrates underwent a rigorous cleaning procedure to eliminate contaminants and ensure optimal film-to-substrate adhesion. The cleaning process involved sequential immersion of the substrates in three different solutions for 10 minutes each: 1-Hydrofluoric acid (HF), 2-Acetone, 3-Ethanol. Hydrofluoric acid was employed to remove the native oxide layer (SiO_2) from the silicon surface, while acetone and ethanol were used to eliminate organic residues. Following the chemical cleaning steps, the substrates were thoroughly rinsed with deionized (D.I.) water to ensure the complete removal of any remaining impurities and organic solvents. This cleaning protocol is critical for achieving uniform, planar growth of ZnO thin films and for establishing strong adhesion to the substrate.

2.2. Solution Preparation

Zinc acetate dihydrate [$Zn(CH_3COO)_2{\cdot}2H_2O$] was employed as the zinc precursor during the deposition process. Precursor solutions were prepared at three distinct molar concentrations: 0.3 M, 0.4 M, 0.5 M [11]. Each solution was

Cite as: A.K. Soatov, A.R. Turayev, A.O. Arslonov, East Eur. J. Phys. 2, 476 (2026), https://doi.org/10.26565/2312-4334-2026-2-53

synthesized by dissolving the appropriate amount of zinc acetate in deionized water. The mixture was continuously stirred until a completely homogeneous solution was achieved. These specific molar concentrations were selected to systematically investigate the influence of precursor concentration on the structural and morphological properties of the resulting ZnO thin films [12,13].

2.3. Deposition Process

The deposition of ZnO thin films was carried out using an ultrasonic nebulizer operating at a frequency of 1.7 MHz. This device atomizes the precursor solution into fine aerosol droplets. The generated droplets were transported into the reaction chamber by a carrier gas flow of oxygen at a constant rate of 500 sccm (standard cubic centimeters per minute). Oxygen was chosen as the carrier gas to facilitate the oxidation of zinc acetate during the pyrolysis process, leading to the formation of the ZnO phase. Silicon substrates were placed on a heated substrate holder, and the temperature was maintained at a constant 400 °C throughout the deposition process. This specific temperature was selected to facilitate the thermal decomposition of the zinc acetate precursor, leading to the formation of high-quality ZnO thin films [14,15].

The thickness of the deposited films for all samples was approximately 80–100 nm. The thickness of both single-layer and multi-layer thin film structures was measured at various incidence angles. Additionally, the optical properties of the film structures, namely the refractive index and extinction coefficient, were determined across the ultraviolet (UV), visible, and infrared (IR) wavelength ranges (240–2500 nm). The thickness of the primary ZnO film layer is 86.64 nm, which is considered an optimal thickness for semiconductor optoelectronics. A surface roughness layer with a thickness of 40.18 nm was also identified, aligning perfectly with the granular structure observed in the SEM images. An interface layer of 6.21 nm and a native SiO_2 oxide layer of 10.50 nm were detected between the ZnO and the Si substrate. At a wavelength of 632.8 nm, the refractive index of the ZnO layer was found to be n = 1.8491. This value is close to the theoretical parameters of ZnO, indicating the high optical density of the synthesized film [16,17].

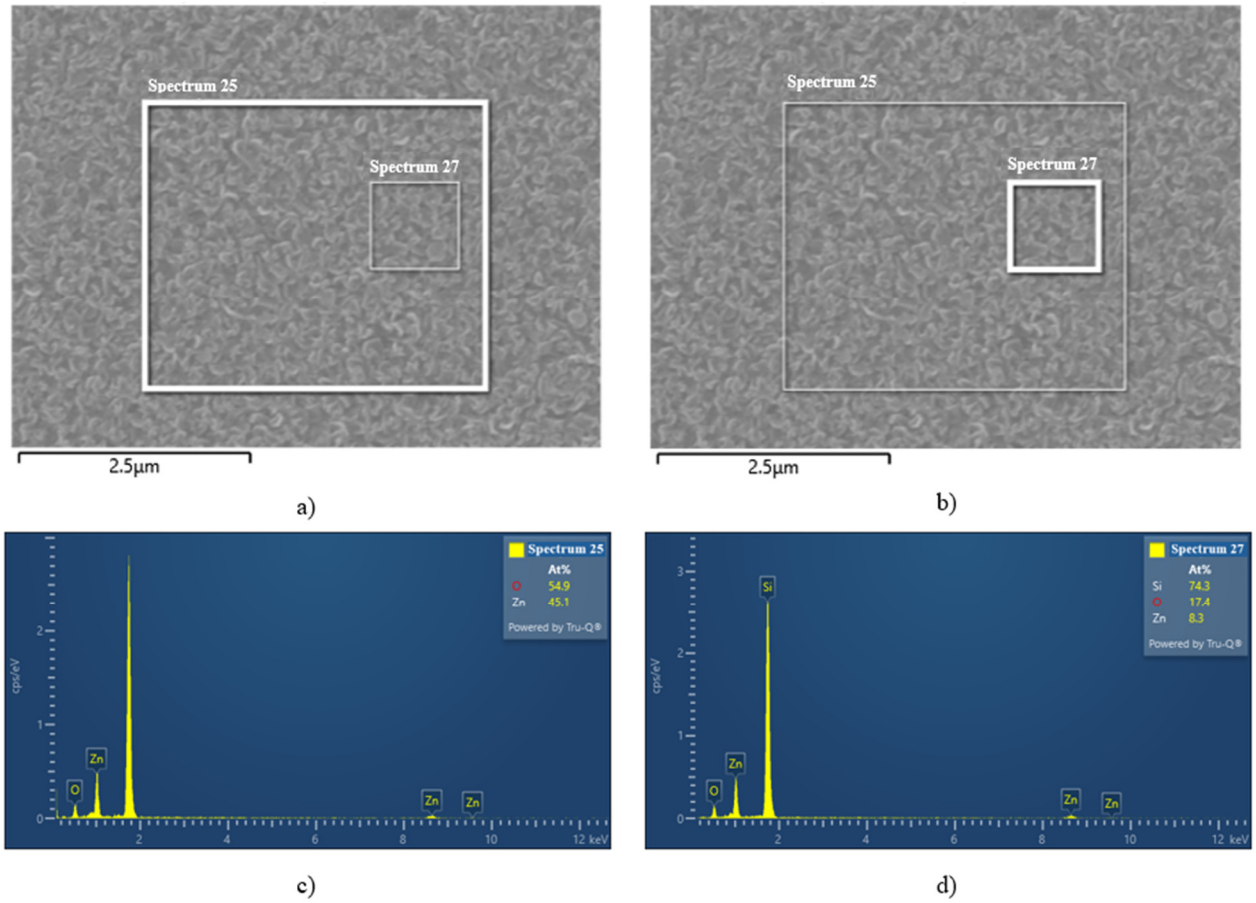

Figure 1. Morphological images and elemental analysis of ZnO thin films obtained using a JEOL JSM-IT510 Scanning Electron Microscope (SEM) (Japan) equipped with an Aztec Advanced (Oxford Instruments) EDX system: a-b) surface morphology of the thin film; c-d) quantitative elemental composition data (EDX spectra)

2.4. Characterization Methods

The morphology and structural properties of the grown ZnO thin films were analyzed using a Scanning Electron Microscope (SEM) to determine surface topography, uniformity, and grain size. Structural analysis was conducted using a Shimadzu X-ray diffractometer (XRD) with CuKα radiation. XRD measurements were performed over the 2θ range of 20° to 60°, enabling identification of crystallographic phases and determination of the film's preferred orientation.

3. RESULTS AND DISCUSSION

3.1. SEM Analysis of ZnO/Si Thin Films

As illustrated by the micrographs in Figure 1, the ZnO thin films synthesized via ultrasonic spray pyrolysis (USP) exhibit a nanostructured, polycrystalline morphology with well-defined grain boundaries. The film surface is composed of closely packed microcrystallites (grains) that are well-interconnected. The size of these grains varies from several tens to hundreds of nanometers, which is in good agreement with the crystallite size of 481 Å determined from the previous XRD analysis. The film surface appears dense and continuous across the entire substrate area. This is a critical physical indicator for ensuring stable electrical conductivity in semiconductor devices. When the growth mechanism and orientation are analyzed alongside the XRD results, several conclusions can be drawn. The shape and alignment of the grains suggest a preferential vertical growth orientation relative to the substrate, typically along the c-axis. This granular morphology, resulting from droplet evaporation followed by crystallization during the USP process, is reflective of the high surface energy inherent to ZnO. The SEM analysis shown in Figure 1(a, b) demonstrates that the ZnO films grown on the Si substrate are well-formed, low in defects, and nanostructured, consistent with established scientific literature. The strong correlation between the morphological (SEM), structural (XRD/Raman), and optical (UV-Vis) analysis results scientifically confirms the high quality and stability of the film's crystal lattice. Furthermore, while the SEM images highlight the dense packing of the grains, the EDX analysis confirms the stoichiometric purity of the elemental composition [18,19].

Elemental Analysis (EDX)

The energy-dispersive X-ray (EDX) spectra confirm the chemical purity and stoichiometry of the synthesized samples. As shown in the spectra of Figures 1(c, d), only peaks corresponding to Zn (zinc), O (oxygen), and Si (silicon) from the substrate were observed. The absence of foreign impurities demonstrates the high selectivity and cleanliness of the ultrasonic spray pyrolysis (USP) process. In Spectra 25, the atomic percentages (At.%) of Zn and O are close to a 1:1 ratio (e.g., 45.1% Zn and 54.9% O). The slight excess of oxygen can be attributed to atmospheric absorption or surface oxidation effects. Furthermore, the high intensity of the Si signal (74.3%) in Spectra 27 indicates either localized thinning of the film at these points or electron-beam penetration through the thin film to the underlying substrate [20].

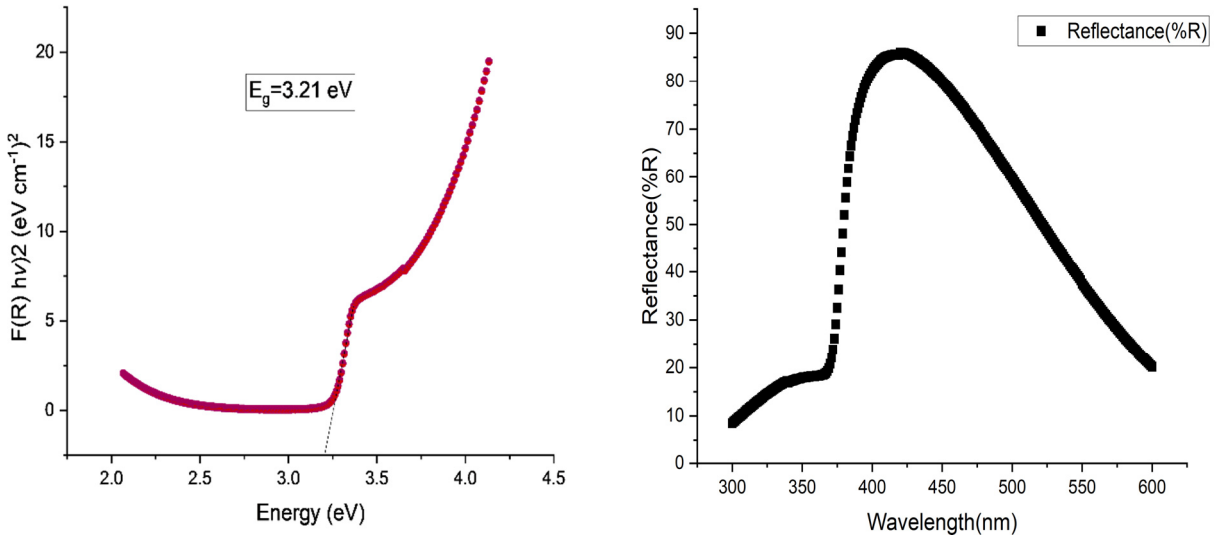

Figure 2. (a) Determination of the optical bandgap energy and (b) dependence of the reflectance coefficient on the wavelength, measured using a YOKE Focus on Lab M601S-X Spectrophotometer

3.2. Reflectance Spectrum and Optical Bandgap Analysis

Spectrophotometric measurements were employed to evaluate the optical characteristics of the synthesized ZnO thin films. Figure 2b illustrates the reflectance spectrum as a function of wavelength (λ), where a sharp increase in the reflectance index is observed near the absorption edge in the 370–380 nm range. This behavior corresponds to the fundamental absorption edge characteristic of ZnO. In the visible region (400–450 nm), the reflectance reaches a maximum value of approximately 85%, indicating high optical quality and excellent transparency (low absorption) for visible electromagnetic waves. The spectral characteristics in the 300–370 nm range confirm the material's strong absorption of ultraviolet (UV) radiation, which may be influenced by hydroxyl groups and intrinsic defects. To determine the optical bandgap energy, a Tauc plot of $[F(R)*hv]^2$ versus photon energy (hv) was constructed based on experimental data [21]. By extrapolating the linear portion of the curve to the energy axis in Figure 2a, the bandgap was calculated as E_g = 3.21 eV. While this value is close to the standard bulk ZnO bandgap of 3.37 eV, the observed redshift to 3.21 eV can be attributed to intrinsic defects, grain-size effects, or lattice strain associated with the Si substrate during the USP process. The linear nature of the plot confirms the presence of direct allowed electronic transitions in the synthesized ZnO films [22].

3.3. Structural Characterization and Crystallite Size Analysis of Zinc Oxide (ZnO)

The X-ray diffraction (XRD) pattern presented in Figure 3 fully corresponds to the hexagonal wurtzite structure of zinc oxide. The primary diffraction peaks observed at 2θ angles of 31.75°, 34.43°, and 36.25° are indexed to the **(**100), (002), and (101) crystallographic planes of the ZnO lattice, respectively. The structural properties of the ZnO thin films were characterized using a high-resolution X-ray diffractometer equipped with a Cu Kα radiation source (λ= 1.5406 Å). The measurements were performed in the Bragg-Brentano (BB) geometry using a D/teX Ultra 250 high-speed detector. To ensure high data quality, a K_β filter was utilized to eliminate secondary radiation. The diffraction patterns were recorded in the 2θ range of 20° to 60° with a step size of 0.01° and a scanning speed of 3.00 °/min. The X-ray diffraction (XRD) analysis confirms that the synthesized ZnO thin films possess a hexagonal wurtzite structure. The dominant diffraction peak, exhibiting the maximum intensity (100%), was observed at 2θ = 34.43°, corresponding to the (002) crystallographic plane. This finding indicates a strong preferred orientation (texture) along the c-axis, perpendicular to the substrate surface. The preferential growth along the (002) direction is a hallmark of high-quality ZnO thin films deposited on silicon substrates via ultrasonic spray pyrolysis (USP). Furthermore, the average crystallite size (D), estimated using the Scherrer formula, was found to be approximately 48 nm. This size suggests that the material is approaching the quantum-scale effect regime, which is beneficial for enhanced optoelectronic performance.

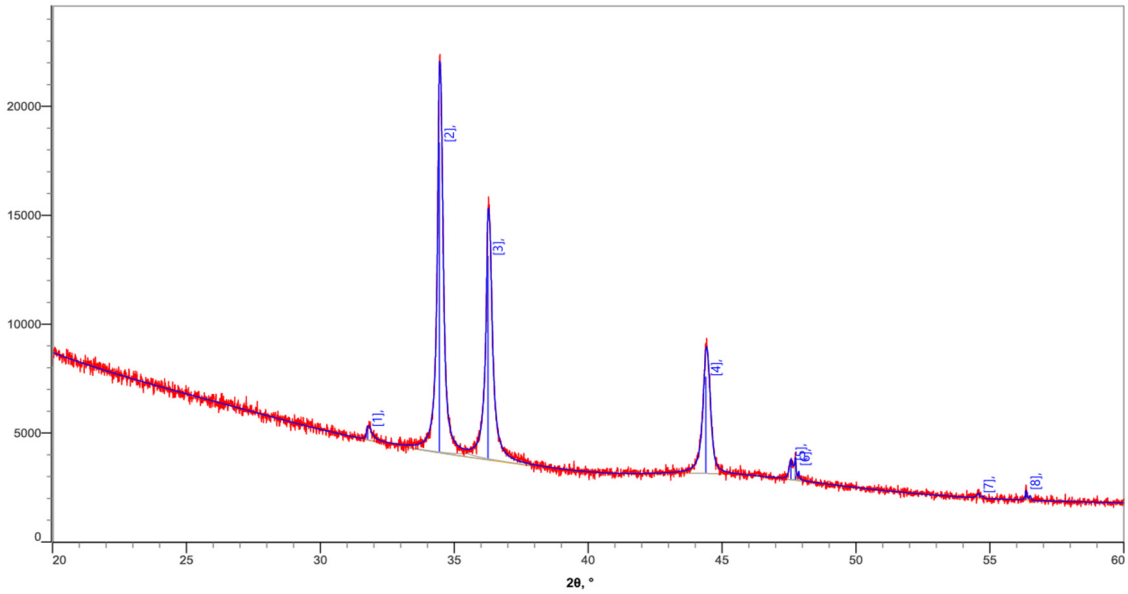

Figure 3. X-ray diffraction (XRD) patterns of the ZnO thin films grown on Si substrates

The high intensity and narrow full-width at half-maximum (FWHM) of the (002) peak (2θ = 34.43°) further demonstrate that the ZnO crystals grew in an ordered, vertical fashion on the Si substrate. The strong correlation between the X-ray structural data and the vibrational spectroscopy (Raman) results provides conclusive evidence of the high crystalline quality and structural integrity of the USP-grown ZnO thin films. The crystalline structure and phase purity of the ZnO thin films were characterized using X-ray diffraction (XRD). As shown in Figure 4, the diffraction patterns exhibit well-defined peaks that are in excellent agreement with the standard hexagonal wurtzite structure of ZnO (JCPDS card no. 36-1451). The most prominent diffraction peak is observed at 2θ = 34.43°, corresponding to the (002) plane. The high intensity of this peak relative to the (100) and (101) reflections indicates that the films possess a strong *c*-axis preferred orientation perpendicular to the substrate surface. This vertical alignment is crucial for enhancing the electrical and piezoelectric properties of the films. The average crystallite size (D) was estimated to be approximately 48 nm using the Scherrer formula:

$$D = \frac{0.9\lambda}{\beta cos\theta}$$

where λ is the X-ray wavelength (1.5406 Å), θ is the Bragg angle, and β is the full width at half maximum (FWHM) of the (002) peak. The relatively narrow FWHM values confirm the high crystalline quality and the successful growth of nanostructured ZnO via the ultrasonic spray pyrolysis method [23].

The crystalline quality of the synthesized ZnO thin films was further evaluated by analyzing the peak intensity and the full width at half maximum (FWHM) of the (002) diffraction plane. As shown in the XRD patterns, the (002) peak exhibited a remarkably high intensity of 14,230 counts per second (cps). The narrowness of the diffraction peaks, characterized by an FWHM of 0.18°, signifies a high degree of crystallinity and a low concentration of lattice defects or internal strain within the ZnO matrix. The average crystallite size (D) was calculated using the Scherrer formula, yielding values of approximately 481 Å (48 nm) and 474 Å (47 nm) for different sampling points. These dimensions confirm that the USP-grown ZnO films are characterized by a well-defined nanostructured morphology.

Table 1. Detailed XRD Structural Parameters for ZnO Thin Films

no.	2θ (°)	d-spacing (Å)	Height (counts/s)	FWHM (°)	Int. Int. (counts/s)	Int. Width (W°)	Size (Å)	Norm. Int. (%)
1	31.759(8)	2.8153(7)	580(18)	0.14(3)	141(13)	0.24(3)	630(116)	3.62
2	34.436(3)	2.60231(19)	14230(215)	0.180(3)	3906(18)	0.274(5)	481(8)	100.00
3	36.250(3)	2.47608(18)	9352(175)	0.184(5)	2885(17)	0.308(8)	474(13)	73.86
4	44.386(7)	2.0393(3)	4432(105)	0.257(6)	1594(17)	0.360(12)	348(8)	40.80
5	47.557(14)	1.9104(5)	844(31)	0.140(17)	179(31)	0.21(4)	646(79)	4.59
6	47.725(3)	1.90410(12)	636(22)	0.042(9)	34(23)	0.05(4)	2173(492)	0.87
7	54.575(13)	1.6802(4)	191(9)	0.12(4)	29(8)	0.15(5)	777(267)	0.75
8	56.327(12)	1.6320(3)	445(19)	0.071(15)	44(6)	0.099(19)	1321(279)	1.13

The correlation between high peak intensity and the nanometric crystallite size indicates that the ultrasonic spray pyrolysis process at 400°C successfully facilitates the formation of a stable, high-quality crystal lattice, suitable for high-performance optoelectronic applications. The quantitative structural data summarized in Table 1 provides a comprehensive insight into the crystalline quality of the USP-deposited ZnO thin films. The diffraction peak at 2θ = 34.436° is the most dominant, with a normalized intensity of 100.00%, which corresponds to the (002) reflection plane of the hexagonal wurtzite phase. The high crystalline integrity of the films is further evidenced by the high peak intensity (14,230 counts/s) and relatively small full width at half maximum (FWHM = 0.180°) for the (002) reflection. The average crystallite size for the major peaks – (002) and (101) – was calculated to be 481 Å and 474 Å, respectively. Interestingly, the diffraction peak at 2θ = 47.725° exhibits an exceptionally narrow FWHM (0.042°). This yields a significantly larger local crystallite size of 2173 Å, despite its relatively low normalized intensity of 0.87%. These structural parameters indicate that the films are highly ordered and nanostructured. The stability of the *d*-spacing values (e.g., $d = 2.602$ Å for the 002 plane) confirms the successful formation of the ZnO lattice on the Si substrate with minimal parasitic phases or impurities [24].

CONCLUSIONS

The analytical results demonstrate that the investigated samples are pure-phase, polycrystalline zinc oxide with hexagonal symmetry, predominantly textured along the (002) plane. Such a structural configuration is characteristic of high-quality thin films and nanopowders utilized in optoelectronics and sensor technologies. Based on the ZnO thin films grown on Si substrates via the ultrasonic spray pyrolysis (USP) method, X-ray diffraction (XRD) analysis confirmed a hexagonal wurtzite phase with a high degree of crystallinity. The preferred orientation along the (002) plane (2θ = 34.436°) signifies ordered growth along the c-axis of the crystal lattice. The average crystallite size, determined by the Scherrer formula, ranges between 34 nm and 64 nm. SEM and ellipsometric analyses revealed a continuous, granular morphology. The geometric thickness of the film was measured at 86.64 nm, with a surface roughness of 40.18 nm. A refractive index of n = 1.8491 (at λ = 632.8 nm) reflects the high optical density of the material. EDX analysis verified high chemical purity and stoichiometric stability (Zn≈45.1 At. %, O ≈54.9 At. %). The absence of secondary phases or impurities was further corroborated by the characteristic E_2(high) (437 cm^{-1}) Raman mode. Spectrophotometric analysis determined a direct optical bandgap of $E_g = 3.21$ eV. The samples exhibited high reflectance (~85%) and transparency in the visible region, with a sharp absorption edge in the ultraviolet (UV) spectrum.

In summary, the synthesized ZnO/Si thin films – characterized by their nanostructured nature, excellent crystalline quality, and optimal optical parameters – represent promising active layers for modern optoelectronic devices, particularly third-generation solar cells and high-sensitivity gas sensors.

ORCID

Azim K. Soatov, https://orcid.org/0009-0004-0375-2889; **Abdumajit R. Turayev,** https://orcid.org/0009-0006-7635-3162;
Azamat O. Arslonov, https://orcid.org/0009-0000-4817-8770

REFERENCES

[1] Y.A. Odedunmoye, I.T. Bello, O.K. Adedokun, M.O. Awodele, and A.A. Awodugba, "Morphological and optical characteristics of ZnO and F: ZnO thin films by a sol-gel spin coating technique," Asian Journal of Physics and Chemical Sciences, **6**(2), 1-11 (2018). https://doi.org/10.9734/AJOPACS/2018/42421

[2] Ü. Özgür, Ya.I. Alivov, C. Liu, A. Teke, M.A. Reshchikov, S. Doğan, V. Avrutin, *et al*. "A comprehensive review of ZnO materials and devices," Journal of Applied Physics, **98**(4), 041301 (2005). https://doi.org/10.1063/1.1992666

[3] C. Klingshirn, *Zinc Oxide: From Fundamental Properties Towards Novel Applications*, (Springer Science & Business Media, 2012). https://doi.org/10.1007/978-3-642-10577-7

[4] Z.L. Wang, "Zinc oxide nanostructures: Growth, properties and applications," Journal of Physics: Condensed Matter, **16**(25), R829-R858 (2004). https://doi.org/10.1088/0953-8984/16/25/R01

[5] A.V. Babalola, V. Oluwasusi, V.A. Owoeye, J.O. Emegha, D.A. Pelemo, A.Y. Fasasi, and S. Yusuf, "Effect of tin concentrations on the elemental and optical properties of zinc oxide thin films," Heliyon, **10**(1), e23190 (2024). https://doi.org/10.1016/j.heliyon.2023.e23190

[6] T.P. Rao, M.S. Kumar, S.A. Angayarkanni, and M. Ashok, "Effect of stress on optical band gap of ZnO thin films with substrate temperature by spray pyrolysis," J. Alloys Compd. **485**(1–2), 413–417 (2009). https://doi.org/10.1016/j.jallcom.2009.05.116

[7] M.R. Wagner, G. Callsen, J.S. Reparaz, J.-H. Schulze, R. Kirste, M. Cobet, I.A. Ostapenko, *et al*. "Bound excitons in ZnO: Structural defect complexes versus shallow impurity centers," Physical Review B, **84**, 035313 (2011). https://doi.org/10.1103/PhysRevB.84.035313
[8] N.L. Tarwal, A.V. Rajgure, A.I. Inamdar, R.S. Devan, I.Y. Kim, S.S. Suryavanshi, and P.S. Patil, "Growth of multifunctional ZnO thin films by spray pyrolysis technique," Sensor Actuator Phys. **199**, 67–73 (2013). https://doi.org/10.1016/j. sna.2013.05.003
[9] K.E. Knutsen, A. Galeckas, A. Zubiaga, F. Tuomisto, G.C. Farlow, B.G. Svensson, and A.Yu. Kuznetsov, "Zinc vacancy and oxygen interstitial in ZnO revealed by sequential annealing and electron irradiation," Physical Review B, **86**(12), 121203 (2012). https://doi.org/10.1103/PhysRevB.86.121203
[10] S.H. Ribut, C.A.C. Abdullah, and M.Z.M. Yusoff, "Investigations of structural and optical properties of zinc oxide thin films growth on various substrates," Results Phys. **13**, 102146 (2019). https://doi.org/10.1016/j.rinp.2019.02.082
[11] A. Arslanov, Sh. Yuldashev, N. Botirova, R. Nusretov, J. Murodov, and J. Xudoyqulov, "Impact of Precursor Molar Concentration on the Structural and Optical Properties of ZnO Thin Films Synthesized by Ultrasonic Spray Pyrolysis," Physical Science International Journal, **29**(1), 29-35 (2025). https://doi.org/10.9734/psij/2025/v29i1871
[12] D.C. Look, "Recent advances in ZnO materials and devices," Materials Science and Engineering: B, **80**(1-3), 383-387 (2001). https://doi.org/10.1016/s0921-5107(00)00604-8
[13] C. Jagadish, and S.J. Pearton, *Zinc Oxide Bulk, Thin Films and Nanostructures*, (Elsevier, 2006). https://doi.org/10.1016/B978-0-08-044722-3.X5000-3
[14] L. Znaidi, "Sol–gel deposition of ZnO thin films: A review," Materials Science and Engineering: B, **174**(1-3), 18-30 (2010). https://doi.org/10.1016/j.mseb.2010.07.001
[15] D.K. Schroder, *Semiconductor Material and Device Characterization*, (John Wiley & Sons, 2006). https://doi.org/10.1002/0471749095
[16] G.E. Jellison Jr, and L.A. Boatner, "Optical functions of ZnO determined by generalized ellipsometry," Physical Review B, **58**(7), 3581 (1998). https://doi.org/10.1103/physrevb.58.3586
[17] H. Fujiwara, *Spectroscopic Ellipsometry: Principles and Applications*. (John Wiley & Sons, 2007). https://doi.org/10.1002/9780470060193
[18] S. Roguai, and A. Djelloul, "Structural, microstructural, and optical properties of ZnO thin films prepared by spray pyrolysis," Algerian Journal of Renewable Energy and Sustainable Development, **4**(1), 94-100 (2022). https://doi.org/10.46657/ajresd.2022.4.1.9
[19] A.Q. Soatov, and A.R. Turaev, "Pressure-induced phase transitions and memristive behavior in Mn- and Co-doped ZnO oxide structures," Scientific Reports of Bukhara State University, **12**(129), 288-292 (2025).
[20] V.K. Devanarayanan, S. Deepa, J. Jassi, and Arshad Salim, "Spray-pyrolysed tin doped zinc oxide thin films-analysis based on microstructural, optical and morphological characterizations," Results in Surfaces and Interfaces, **20**, 100624 (2025). https://doi.org/10.1016/j.rsurfi.2025.100624
[21] T.P. Rao, and M.C. Santhoshkumar, "Effect of thickness on structural, optical and electrical properties of nanostructured ZnO thin films by spray pyrolysis," Appl. Surf. Sci. **255**(8), 4579–4584 (2009). https://doi.org/10.1016/j.apsusc.2008.11.079
[22] J.X. Murodov, Sh.U. Yuldashev, A.O. Arslanov, N.U. Botirova, R.Sh. Sharipova, and J.Sh. Khudoykulov, "NDR in Co:SnO_2 Memristors: Nanocluster Control for Enhanced Performance," Crystal Growth & Design, **26**(1), 317-321 (2026). https://pubs.acs.org/10.1021/acs.cgd.5c01258
[23] F. Zahedi, R.S. Dariani, and S.M. Rozati, "Structural, optical and electrical properties of ZnO thin films prepared by spray pyrolysis: effect of precursor concentration," Bull. Mater. Sci. **37**(3), 433–439 (2014). https://doi.org/10.1007/s12034- 014-0696-8
[24] J.X. Murodov, Sh.U. Yuldashev, A.O. Arslanov, N.U. Botirova, J.Sh. Xudoyqulov, R.Sh. Sharipova, R.A. Nusretov, *et al*., "Resistive Switching Behavior of SnO_2/ZnO Heterojunction Thin Films for Non-Volatile Memory Applications," East Eur. J. Phys. (3), 348−352 (2025). https://doi.org/10.26565/2312-4334-2025-3-34

СТРУКТУРНІ, МОРФОЛОГІЧНІ ТА ОПТИЧНІ ВЛАСТИВОСТІ ТОНКИХ ПЛІВОК ZnO, ВИРОЩЕНИХ НА ПІДКЛАДКАХ Si ЗА ДОПОМОГОЮ УЛЬТРАЗВУКОВОГО РОЗПИЛЮВАЛЬНОГО ПІРОЛІЗУ

Азім К. Соатов[1], Абдумаджит Р. Тураєв[1], Азамат О. Арслонов[2]
[1]Центр розвитку нанотехнологій, Національний університет Узбекистану
[2]Кафедра фізики, Національний університет Узбекистану, Ташкент 100174, Узбекистан

На основі наукових джерел, що представляють сучасні технології виготовлення напівпровідникових приладів та методи вирощування, а також вплив зовнішніх факторів на зразки ZnO було оцінено за допомогою різних підходів. У цій роботі тонкі плівки ZnO були вирощені на підкладках Si за допомогою методу ультразвукового розпилення (USP). Було досліджено фізичні характеристики отриманих зразків, зокрема енергію оптичної забороненої зони та лазерну раманівську спектроскопію *in situ*. Основною метою цього дослідження був синтез тонких плівок ZnO з точною нанометричною товщиною на кремнієвих (Si) підкладках, а також дослідження впливу температури підкладки, складу прекурсора та швидкості випаровування. Використовуючи еліпсометрію, рентгенівську дифракцію та скануючу електронну мікроскопію (CEM), ми охарактеризували товщину плівки, структуру кристалічної решітки та морфологічну еволюцію під час процесу росту.

Ключові слова: *кремній; оксид цинку; кристалічна структура; молярна концентрація; заборонена зона*